3.2 Cold Spray Equipment

3.2.1 Basics of Cold spray system

Kazuhiko Sakaki
Shinshu University, Faculty of Engineering

3.2.1.1. Principles

Based on the results of study conducted at many researchers over the world, several type of cold spray equipment[1)] have been developed by different companies including ITAM SB RAS(Russia), Kteck corporation (USA), Sulzer Metco（Switzerland), Impact Innovations GmbH (Germany), Plasma Giken Co. Ltd. (Japan), OCPS (Russia) , Centerline (Canada) and others. This section presents a description of the CS equipment, the nozzle design and geometry of cold spray gun. To illustrate the main aspects of cold spray system parameters determination the numerical simulation and experimental data are presented in Paragraph 3.2.2.

A schematic diagram of a cold spray system is shown in Figure 3.13. Cold spray system consists of the following major components:

1) high pressure gas supply (Nitrogen, helium, air or those mixed gases)
2) gas control module
3) resistive coil gas heater and power supply
4) pre-chamber and supersonic nozzle assembly
5) powder feeder (high-pressure type powder feeder for an axially powder injection (A/I), low-pressure type powder feeder for radially powder injection (R/I)

6) process control and data acquisition system

7) robot and its controller.

FIGURE 3.13. Schematic diagram of a cold spray system.

The process gas is introduced through a gas control module to a manifold system containing a gas heater and powder feeder. The high-pressure gas is heated to a preset temperature, often using a coil of an electrical resistance heated tube. The gas is heated *not* to heat or soften spray particles but instead to achieve higher sonic flow velocities, which ultimately result in higher particle impact velocities. The high-pressure gas is introduced into the converging section of a de Laval-type nozzle (i. e., a convergent-divergent nozzle, but convergent-divergent-barrel nozzle in Fig.3.13), the gas is accelerated to sonic in the throat region of the nozzle, and the flow then became supersonic (Mach numbers ranging from 2 to 4) as it expands in the divergent section of the nozzle[2)]. The powder is delivered by a precision metering device called “powder feeder” and typically is injected axially into the center of the high-pressure side of the nozzle intake (axial injection of powder: A/I) (in most case). The powder is accelerated in the divergent and the barrel section of the nozzle, and powder and the gas gush out in the atmosphere and collide with a substrate. And the powder which collided in higher than the critical velocity deposits and forms a coating.

One of the major elements of the cold spray process is the high-speed gas jet, which is governed by gas dynamics. In gas dynamics, supersonic flows are obtained with convergent-divergent (or de Laval) nozzles. Thus, in cold spray, the nozzle is one of the most important components.

3.2.1.2 Cold spray process classification

Table 3.3 shows cold spray process classification. As for the current cold spray system, a pressure of the process gas is classified roughly into **high pressure types** more than 1MPa and two of the following **low-pressure types**. Furthermore, there is the example which I put CS device in a decompression chamber by a researcher, and calls itself “the vacuum cold spray”, but leaves out explanation in the quality dried bonito because I repeat with the aerosol deposition method[3)].

Table 3.3. Classification of cold spray process and device.

High-pressure/low-temperature gas type shown at (a) in Table3.3 is the first generation CS system with less than approximately 600ºC of process gas temperature at nozzle intake. High-pressure/high-temperature gas type shown at (b) is the second generation CS system with high temperature (1,000 ºC) of gas more than (a), and make fireproof metal, such as tantalum and niobium, deposit and improve quality of coating to have improved an adhesion and deposing rate of its coating.

The possibility of obtain coating from the WC/Co composition with use of additional preheater of the powder (i,e., increasing its initial temperature at nozzle intake) in CS system of Taekwang tech[5),14)].

In (a) the high-pressure/low-temperature type CS system, powder size to use was approximately around 5-50μm, and marketing spray powder was not often available because it was smaller than a commercial powder size distribution for conventional thermal spray. There is Kinetic Spray® (only as for the plot type) which improved this fault by nozzle entrance part extension1). The gas flows in the entrance convergent section of the nozzle exhibit a relatively higher temperature and are subsonic; thus, this region is most suitable for heating spray particles, mentioning it later in #3.2.1.4. In the second generation commercial high-pressure/high-temperature type CS system (b), the extension of the entrance convergent section of the nozzle and a higher temperature of the process gas became it the

relatively bigger particle size was available. In addition, the high pressure portable system (c) in Table 3.3 was developed for repair in 2009, too.

New CS device (SISP: Shock-wave Induced Spray Process) such as an explosion spray device (g) in Table 3.3 intermittent continuation-shaped a detonation that researchers of Ottawa University developed in 2005, and they continue this work now[17].

In low-pressure types of (d)-(f) in Table 3.3, Kashirin and colleagues have developed a downstream injection of the powder(R/I)[18], therefore the powder became able to supply to the nozzle by low pressure, and a high-pressure vessel of powder feeder became needless. However it should be noted that this technique results in a subsonic particle beam hence requires a peening agent to hammer the particles deposited onto the substrate, and to form coating. The low-pressure cold spray process yields coatings of selected ductile materials with acceptable coating characteristics, as compared to the high-pressure process which yields coating of almost any materials with highest coating quality [2].

On the other hand, low temperature high-speed flame spray (HVOF) device (h) (Table 3.3) for warm spray process, was developed by researchers[19]at 2000. The temperature of the supersonic gas flow is generated by the combustion of kerosene and oxygen with HVOF flame spray gun which is controlled by diluting the combustion gas with an inert gas such as nitrogen[19]. As for this warm spray, the new model which raised combustion pressure for a further technological advance to 4MPa was developed recently[13]

At all events, determination of a shape and the dimensions of the nozzle is very important rather than elevating temperature and pressure of the process gas to accelerate and heat particles efficiently. This nozzle design and geometry will be explained in the next paragraph.

3.2.1.3. Nozzle design and geometry[20)]

Introduction to nozzle design for cold spray process

As shown before (Chapter 2.1), one of the major characteristics of the cold spray process is the high-speed gas jet, which is governed by gas dynamics. In gas dynamics, supersonic flows are obtained with convergent–divergent (CD) nozzles (or de Laval nozzle), which are used for rocket motors. Rocket motors, including their nozzle design, have been studied and analyzed in detail. While the principal purpose of the design of a rocket motor nozzle is to maximize the thrust, in thermal spraying (including cold spray) the main purpose is to obtain better coating quality[21)–32)].

Cold spray systems employ various kinds of gun nozzle contours, such as CD (or de Laval nozzle) [1), 18), 22) – 30), 32)], convergent–divergent-barrel (CDB)[26), 32)] and convergent-barrel (CB) [26,28),31)].

Previous studies on thermal spraying show that the coating properties are principally determined by the thermal and kinetic energy states of particles upon impact with the substrate. In order to have a balance between these two states, various changes in the design of the high-velocity oxygen fuel (HVOF) gun nozzle have been attempted. However, works concerning the influence of nozzle geometry on the thermal spray process are sparse[21) –23)]. Previously, the effects of throat diameter and exit divergence of the gun nozzle on the HVOF process have been considered[23)]. The combustion gas flow (such as pressure, velocity, temperature and expansion state of gas jet from the nozzle exit), the particle behavior and, therefore, the nature of coatings were found to be significantly influenced by these nozzle parameters. In addition, the effect of the expansion state of the combustion gas jet on the HVOF process was investigated using a diverging nozzle exit. The particle velocity reached a maximum with the

correct expansion state of the gas jet due to an increased gas jet velocity. This resulted in an increase in the bonding strength of the NiCrAlY coating[23].

The nozzle geometry is also important with regard to the cold spray method. In the cold spray method, a coating is formed by exposing a substrate to high-velocity solid-phase particles, which have been accelerated by supersonic gas flow at a temperature much lower than the melting temperature of the feedstock. In this paragraph, the influence of contours(shape), expansion ratio (exit diameter /throat diameter) , nozzle length and cross-sectional shape of nozzle on the cold spray process (i.e., the behavior of the process gas and spray particles) is investigated by experiments and a numerical simulation prior to designing the cold spray equipment and producing coatings. The governing equations of a numerical simulation were shown in Chapter 2.1 and Paragraph 3.2.2 in detail, and, the results of experiments and a numerical simulation are described below.

Nozzle shape influence (modeling results)

Figure 3.14 shows schematic diagrams of the cold spray nozzles used for numerical simulation of gas flow within the nozzles: (a) CB nozzle; (b) CD (or de Laval) nozzle; (c) CDB nozzle. The cross-sections of these nozzles are circular. Nozzle total length l, entrance converging length $l_{conv.}$, entrance diameter d_i, and throat diameter d_t are shown in Table 3.4. The results provided by this simulation could be a little larger than the real values.

FIGURE 3.14. Schematic cross-section diagram of the cold spray nozzles: (a) convergent-barrel nozzle, (b) convergent-divergent nozzle, (c) convergent-divergent-barrel nozzle.

Table 3.4 Cold spray gun nozzle size

The numerical simulation results for the effect of nozzle geometry on gas pressure, velocity of gas, and particles, and temperature of gas and particles are given in Figure 3.15. The cold spray condition data used and the initial conditions are shown in caption of Figure 3.1.5. In this paragraph, the modeling results of the CD nozzle, which is used by typical cold spray devices, (CD nozzle in Figure 3.15) are explained.

FIGURE 3.15 Effect of nozzle geometry on calculated results of (a) nozzle contour, (b) gas pressure, (c) velocity of gas and particle, (d) temperature of gas and particles for nitrogen as the process gas, copper particle (15 μm). Gas initial (stagnation) pressure P_i=3.5 MPa, gas initial temperature T_{gi} =600 K, gas initial velocity U_{gi} =10 m/s, T_{pi} =300 K, particle initial velocity U_{pi} =10 m/s7[26].

The acceleration of the gas takes place predominately in the area of the nozzle throat and in the first third of the diverging section. Here the gas velocity U_g has already reached 85% of its exit velocity. Namely, gas velocity reaches sonic velocity at the nozzle throat and reaches supersonic velocity with the increasing cross-sectional area of the nozzle in the diverging section (see Fig.3.15c). At the same time the gas temperature drops to values far below room temperature as the gas expands in the diverging section of the nozzle. The particle is introduced into the gas flow immediately upstream of the converging section of the nozzle and is accelerated by the rapidly expanding gas. The dwell time of the particle in contact with hot gas is brief, and the temperature of the solid particle at impact remains substantially below the initial gas preheat temperature.

The numerical simulation results of the effect of nozzle geometry on gas pressure, velocity of gas and particles, and temperature of gas and particles are shown on Figures 3.15b, c and d respectively. . It is clearly seen that for the CD nozzle and the CDB nozzle the gas pressure (or density) decreases significantly to a very low value upon leaving the nozzle throat owing to the fast gas expansion (see Fig. 3.15b). On the other hand, for the CB nozzle, the gas pressure is not significantly decreased along

the nozzle up to the exit. Moreover, the oscillation of the gas variables outside the nozzle exit indicates that expansion waves are generated, and those are more obvious for the CB nozzle[26), 28)]. This is due to the fact that at the nozzle exit the high-pressure gas expands sharply to ambient for the CB nozzle, while for the CD and CDB nozzles, the gas has expanded gradually from the throat.

Figure 3.15c shows that the gas velocity increases remarkably to a high value after leaving the nozzle throat with the CD and CDB nozzle, while the velocity is relatively low (sonic velocity) with the CB nozzle. Although the particle velocity with the CB nozzle is lower than that with CD and CDB nozzles, the ratio of the particle velocity to the gas velocity is higher for the CB nozzle. This shows that particles can achieve more effective acceleration with a CB nozzle, because the particle velocity is not only influenced by the driving gas velocity but also by the gas density, as shown in Chapter 2.1. The results demonstrate that the particle velocity at the nozzle exit for the CD nozzle is higher than that for the CDB and CB nozzles. On the other hand, the particle temperature at the nozzle exit for the CB nozzle is higher. The divergent section with the CD nozzle (Fig. 3.14b) is conical. The numerical codes of fluid dynamics, in particular the method of characteristics (MOC), were also used to develop new nozzle designs that allow a more uniform particle acceleration[29), 30)]. According to the MOC, the bell-shaped diverging section nozzle can produce better and more uniform particle acceleration over the diameter of the nozzle cross-section. Using the standard trumpet-shaped nozzle, a copper particle may be accelerated to a velocity of 500 m/s, which is not high enough to allow the bonding of copper. At the same parameter setting using the bell-shaped MOC-designed nozzle, the velocity of a 20 μm copper particle is increased to 580 m/s, which is well above the critical velocity of copper of 550 m/s[30)].

Influence of nozzle expansion ratio[33)]

The spray gun is fitted with a convergent-divergent nozzle (or a conical de Laval nozzle) designed to produce perfectly an expansion gas jet[34], which is supersonic at its exit, and free shock diamonds. Namely, the nozzle exit pressure P_e of the gas fed at varied nozzle intake pressures P_i matches the ambient pressure by changing the nozzle exit diameter d_e. Schlieren photographs illustrating the influence of the expansion ratio of cross-sectional areas at the throat A_t and exit of the nozzle A_e on the expansion state of the gas jet are presented in Figure 3.16. Gas expanded within the diverging section of the nozzle and the expansion state of the gas jet changed from significant under-expansion (Fig. 3.16a) to over-expansion (Figure3.16c) with an increasing expansion ratio.

FIGURE 3.16 Schlieren photograph illustrating the influence of the expansion ratio of the nozzle on the expansion state of nitrogen gas jet without substrate. The expansion ratio A_t / A_e of the gun nozzle: (a)4; (b)9, (c)16. (T_{gi} = room temperature, P_i =3.0 MPa)

Figure3.17 shows the change in the deposition efficiency η (that is experimental value) of cold sprayed copper coatings with a change in the expansion ratio under different nozzle intake gas pressures P_i at T_{gi} = 400 ºC. In the same way, Figure 3.18 shows the change in the deposition efficiency η with a change in the nozzle intake gas pressure for different A_e / A_t ratios at T_{gi} = 300ºC. It was clearly found that the deposition efficiency η increased with an increasing expansion ratio and reached a peak at a particular expansion ratio, and then decreased with a further increase in the expansion ratio under different nozzle intake gas pressures P_i. For example in Figure 3.16, η under P_i = 1.5 MPa reached a peak of 60% when the expansion ratio was 9, and η under P_i = 4.0 MPa reached a peak of 90% when the expansion ratio was around 16. In Figure 3.18 at gas temperature T_{gi} of 300 ºC, η were lower than those at 400 ºC in Figure3.17. Thus, these results show the existence of an optimal expansion ratio, for

which the particle velocity and deposition efficiency are a maximum under a given intake pressure P_i estimated. In addition, the optimal expansion ratio increases with increasing gas pressure P_i. The nozzle intake gas pressure and ratio A_e/A_t of cross-sectional areas at the throat and exit of the gun nozzle affect the deposition efficiency of cold sprayed copper coatings.

FIGURE 3.17 Influence of the expansion ratio of the gun nozzle and gas pressure on the deposition efficiency of cold sprayed copper (10μm) coatings at T_{gi} = 400□,with powder R/I[33].

FIGURE 3.18 Influence of the gas pressure and expansion ratio of the gun nozzle on the deposition efficiency of cold sprayed copper (10μm) coatings at T_{gi} = 300□,with powder R/I[33].

From these experimental results, the expansion ratio of the nozzle maximizing a deposition efficacy each nozzle intake gas pressure P_i in MPa is expressed in equation (3.1).

$$\frac{A_e}{A_t} \geq 1.5P_i + 6.9 \qquad (3.1)$$

Now in the low-pressure cold spray patent[18], the cross-sectional areas of the supersonic nozzle at the juncture of the nozzle and the powder-feeder conduit should be related to the throat area per the following relation, too

$$\frac{S_i}{S_k} \geq 1.3P_0 + 0.8 \qquad (3.2)$$

where S_i is the cross-sectional area of the supersonic nozzle at the juncture of the nozzle and the powder feeder conduit, S_k is the supersonic nozzle throat area, P_0 is the full gas pressure at the supersonic nozzle inlet, expressed in MPa.

3.2.1.4 *Influence of nozzle length*

Assadi et al. (2003) can express a relation of the critical velocity V_{cr} and effect of these parameters in the following simple formula[35]

$$V_{cr} = 667 - 14\rho + 0.08T_m + 0.1\sigma_u - 0.4T_{pi} \quad (3.3)$$

Where $\boldsymbol{\rho}$ is the particle density in g/cm^3, T_m is the melting temperature in °C, σ_u is the ultimate strength of particle in MPa and T_{pi} is the initial particle temperature before impact in °C.

In this formula, particle temperature have significant effects on the critical velocity in cold gas spraying. In other words, the critical velocity V_{cr} decreases with increasing the particle impact temperature T_{pi}, and the particle becomes easy to forms a coating[23), 32)].

The gas flows in the entrance convergent section of the nozzle exhibit a relatively higher temperature and are subsonic; thus, this region is most suitable for heating spray particles. The effect of the nozzle entrance convergent section length $l_{conv.}$ on the cold spray deposition efficiency[37)] is shown on Figure3.19, which depicts the dependence of the deposition efficiency on l_{conv} . Deposition efficiency of both copper and titanium increase with increasing the length of the convergent section of the nozzle. But deposition efficiency with type C nozzle adding cylinder on this side of convergent section decrease, because big Reynolds number may make the gas flow turbulent in cylinder. Deposition efficiency of copper coating reached a peak of 95% with A150 and B150 nozzle.

FIGURE 3.19 Effects of entrance convergent section length of nozzle type A(Converging-diverging nozzle), B(Converging-diverging -barrel nozzle) and C(Cylinder-converging-diverging -barrel nozzle) on the depositing efficiency with copper(mean particle size: 13μm) and titanium powder(mean particle size: 25μm) with nitrogen gas initial (stagnation) pressure P_i=3.0 MPa, gas initial temperature T_{gi} =350℃ [32)].

Influence of Nozzle cross-sectional shape

In the cold spray process, cross-sectional shape of the nozzle has a significant effect on spray pattern of coatings (Sakaki et al., 2014). There are a rectangular and a circular cross-sectional shapes on the cold spray nozzles. It is known that spray pattern of the rectangular spray nozzle is wider than that of the circular one. Accordingly, the rectangular nozzle has better capacity than circular one at cold spraying passes of a constant width. However, commercially cold spray nozzle is mostly circular. The goal of this paragraph is to establish a design for the cold spray gun nozzle in order to gain a flatter spray pattern of coatings. Sakaki et al., 2014 performed the CFD numerical simulation and experiments to study the effect of cross sectional shape of cold spray nozzle on spray pattern of copper coatings. The CS nozzle shapes are shown on Fig.3.20.

Figure 3.20 Schematic diagrams of rectangular and circle cold spray nozzles[38].

Two different rectangular nozzles, such as a converging-diverging-barrel (CDB) rectangular nozzle with expansion ratio of 6.1 and converging-diverging (CD) rectangular nozzle with expansion ratio of 6.1, 11.2 and 15.0were made to compare their spraying parameters with those of the circular nozzle. It is found that the spray pattern fabricated by CD rectangular nozzle has become more flat, uniform and wider than that of circular nozzle. However, a spray pattern of coating with the CDB rectangular nozzle has a concave shape. The numerical simulation results reveal that at divergent section, the gas axial velocity and the velocity along a nozzle width axis $\boldsymbol{y}$ ($\boldsymbol{V_{Gy}}$) are different for the CDB rectangular nozzle and CD rectangular nozzle. The velocity along a nozzle width axis $\boldsymbol{V_{Gy}}$ is about 150m/s for CDB

rectangular nozzle, whilst V_{Gy} = 30m/s for the CD rectangular nozzle. It is defined that the optimized expansion ratio of CD rectangular nozzle is of about 11.2.

References

1） Alkimov Anatoly P., Kosarev Vladimir F. , Nesterovich Nikolai I., Papyrin Anatoly N. and Shushpanov Mikhail M., Gas Dynamic Spraying Method for Applying a Coating, U. S. Patent 5302414, 12 April 1994.

2） Edit by Tucker, Jr. Robert C., "*ASM Handbook Vol.5A Thermal Spray Technology*" (Materials Park: ASM international, 2013), 55-56.

3） Akedo, J., Roomtemrerature impact consolidation (RTIC) of fine ceramic powder by aerosol deposition method and applications to microdevice, *J. Thermal Spray Technol.*, 17(2), 181-198, 2008.

4） http://www.sulzer.com/en/Products-and-Services/Coating-Equipment/Thermal-Spray/Spray-Guns/Cold-Spray (accessed March 14, 2014 ; This website is unavailable now).

5） http://www.a-tkt.co.kr/home/html/index.php# (in koria) (accessed August 27, 2015).

6） http://www.impact-innovations.com/en/coldgas/cg_index_en.html (accessed August 27, 2015).

7） http://www.plasma.co.jp/en/products/coldspray.html (accessed August 27, 2015).

8） http://www.licenz.ru/eng/tech_dymet.html (accessed August 27, 2015).

9） http://www.supersonicspray.com/en/cold_spray?pg=SE20000 (accessed August 27, 2015).

10） http://www.inovati.com/KMequipment/KM%20systems/systems-specs.php (accessed August 27, 2015).

11） http://www.medicoat.com/thermal-spray-systems/cold-spray/ (accessed August 27, 2015).

12） Jodoin, B., Richer, P., Berube, G., L Ajdelsztajn, Pulsed-Gas Dynamic Spraying: Process analysis, development and selected coating examples, *Surface and Coatings Technology*, 201, 7544-7551,2007.

13） Molak, RM, Araki,H., Watanabe, M., Katanoda,H.,Warm Spray Forming of Ti-6Al-4V, *J. Thermal Spray Technol.*, 24(1-2), 197-212, 2014.

14） Kim, H. J., Lee, C., H., Hwang, S., H., Fabrication of WC–Co coatings by cold spray deposition, *Surface & Coatings Technol.*, 191,335 – 340, 2005.

15） Steenkiste T. Van, Smith J.R., Teets R.E., Moleski J.J., and Gorkiewicz D.W. ,Kinetic Spray Coating Method and Apparatus, U.S. Patent 6 139 913, Oct. 31, 2000.

16） Steenkiste T. Van, Smith J.R., Evaluation of Coatings Produced via Kinetic and Cold Spray Processes, *J. Thermal Spray Technol.*, 13(2), 274-282, 2004.

17） Yandouzi B. M., Jodoin , P. ,Richer, Jodoin. B. ,Pulsed-Gas Dynamic Spraying: Process analysis, development and selected coating examples, *Surface and Coatings Technology*, 201, 7544-7551, 2007.

18） Kashirin A.I, , Klyuev O.F. and Buzdygar T.V.,Apparatus for gas-dynamic coating, U.S. Patent 6402050, June 11, 2002.

19） Kuroda, S., Watanabe, M., Kim, K. H. and Katanoda, H., Current Status and Future Prospects of Warm Spray Technology, *J. Thermal Spray Technol.*, 20(4), 653-676, 2011.

20） Edited by Champagne V.K., "*the cold spray materials deposition process - fundamentals and applications*-" (Cambridge, England: Woodhead publishing, 2007), 117-126.

21） Hackette, C. M. and Settles, G. S., The Influence of Nozzle Design on HVOF Spray Particle Velocity and Temperature, *Thermal Spray Science & Technology*, C. C. Berndt and S. Sampath, Ed, ASM International, Material Park, OH, 1995, 135-140.

22） Kopiola, K., Hirvonen, J.P., Laas,L. and Rossi,F. ,The Influence of Nozzle design on HVOF Exit Gas Velocity and Coating Microstructure, *J. Thermal Spray Technology*, 1997, l6 (4), 469-474.

23） Sakaki, K. and Shimizu, Y., Effect of Increase in Entrance Length of Gun Nozzle on HVOF and Cold Spray Process, *J. Thermal Spray Technology*, 2001,10 (3) 487-496.

24） Gilmore, D.L., Dykhuizen, R.C., Neiser, R.A., Romer, T.J. , Smith, M.F., Particle Velocity and deposition Efficiency in Cold Spray Process, *J. Thermal Spray Technology*, 1999,8 (4) ,576-582.

25） Stoltenhoff ,T., Kreye, H., Richter, H.J., An analysis of the cold spray process and its coatings, *J. Thermal Spray Technology*, 2002,11 (4), 542-550.

26） Sakaki, K. , Huruhashi,N., Tamaki K. and Shimizu, Y., Effect of nozzle geometry on cold spray process, *International Thermal Spray Conference*, 2002 , Essen, Germany, 385-389.

27） Han,T., Zhabo, Z., Gillispie, B. A. and Smith, J. R., Effect of spray conditions on coating formation by the kinetic spray process, *J. Thermal Spray Technology*, 2005,14(3) 373-383.

28） Wen-Ya Li, Chang-Jiu Li, Optimal design of a novel cold spray gun nozzle at a limited space, *J. Thermal Spray Technology*, 2005,14(3) ,391-396.

29） Heinrich,P., Kreye, H., and Stoltenhoff, T., Laval nozzle for thermal and kinetic spraying, U.S. Patent 0001075 A1, January 6, 2005.

30） Gaertner,F., Stoltenhoff, T., Schmidt,T. and Kreye, H. ,the cold spray process and its potential for industrial applications, *J. Thermal Spray Technology*, 2006,15(2), 223-232.

31） Wen-Ya Li, Hanlin Liao, Hong-Tao Wang, Chang-Jiu Li, Ga Zhang and C. Coddet ， Optimal design of a convergent-barrel cold spray nozzle by numerical method， A*pplied Surface Science*, 2006,253(2), 708-713.

32） Sakaki, K., Takahata, M., Takeda, K., Shinkai, S., Hosono, T., and Shimizu, Y., Effect of the increase in the entrance convergent section length and geometry of the gun nozzle on properties of cold sprayed copper and titanium coatings, *Proceedings of International Thermal Spray Conference*, 2008, Maastricht, Netherlands.

33） Sakaki, K., Takeda, K., Takada, K., Hosono, T., and Shimizu, Y., Influence of the expansion ratio of the gun nozzle and gas pressure on properties of cold sprayed copper coatings, *Proceedings of the 3rd JSME/ASME International Conference on Materials Processing,* 2008, Illinois, USA, MSEC_ICM&P2008-72015.

34）Sakaki, K., Shimizu, Y. , Gouda Y., and Devasenapathi A., Effect of Gun Nozzle Geometry on High Velocity Oxygen-Fuel (HVOF) Thermal Spraying Process , in Thermal Spray: *Meeting the Challenges of 21st Century*, C. Coddet, ed., ASM International, Materials Park, OH, 1998, 445-450.

35） Assadi, H., Ga¨rtner, F., Stoltenhoff, T., Kreye, H., Bonding mechanism in cold gas spraying, *Acta Materialia* 51 (2003) ,4379–4394.

36） Papyrin, A., *Cold Spray Technology*, (Oxford: Elsevier, 2007), 217-218.

37） The leaflet of Kinetics 4000® Cold spray system by Cold Gas Technology GmbH, 05 May 2006.

38） Sakaki, K., Akashi, T., Hosono, T., Influence of cross sectional shape of cold spray nozzle, *Proceedings of the JSME/ASME 2014 International Conference on Materials and Processing, ICMP2014*, Detroit, Michigan, USA, June 9-13, 2014, ICMP2014-4961.

Manuscript 3.2.1. Figure captions –figures - tables

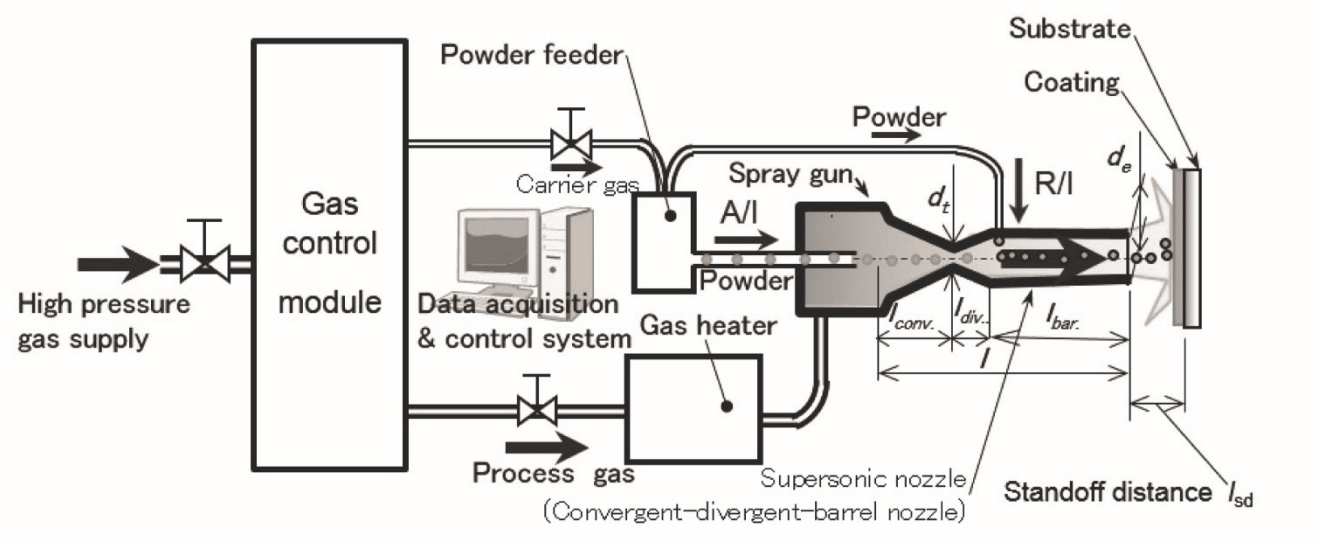

Fig. 3.13. Schematic diagram of a cold spray system.

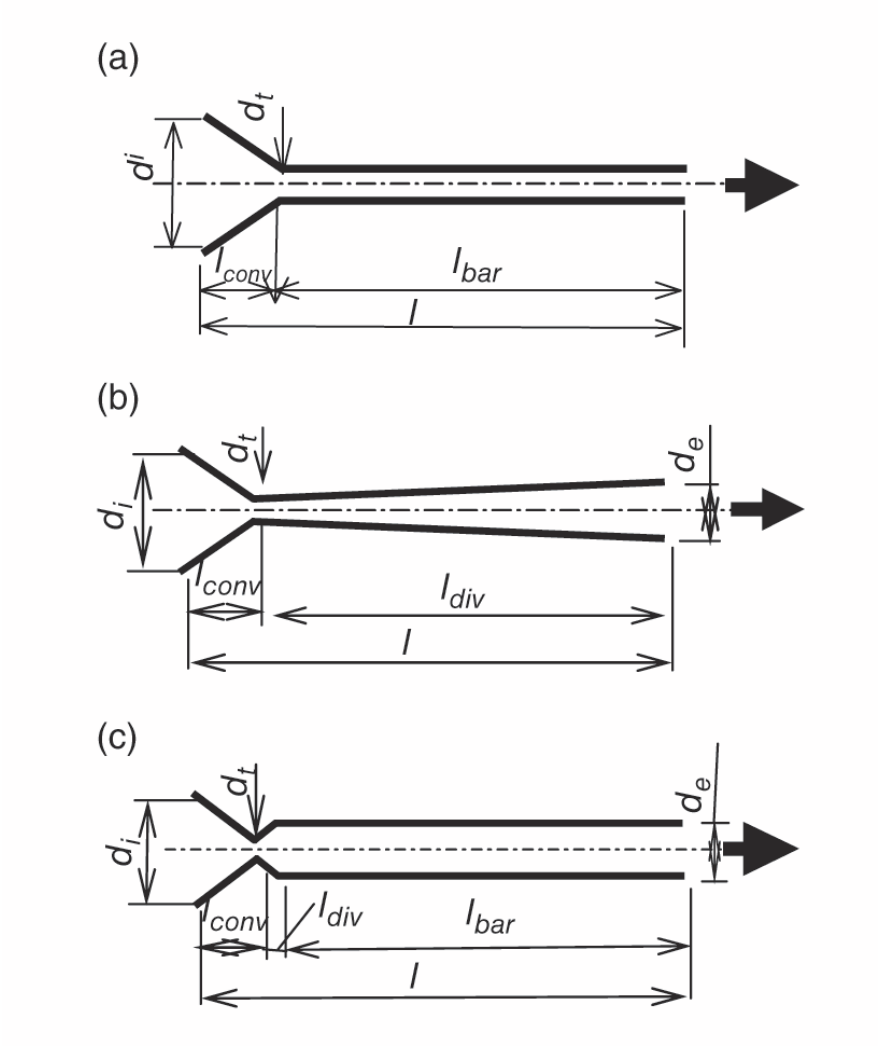

FIGURE 3.14. Schematic cross-section diagram of the cold spray nozzles: (a) convergent-barrel nozzle, (b) convergent-divergent nozzle, (c) convergent-divergent-barrel nozzle.

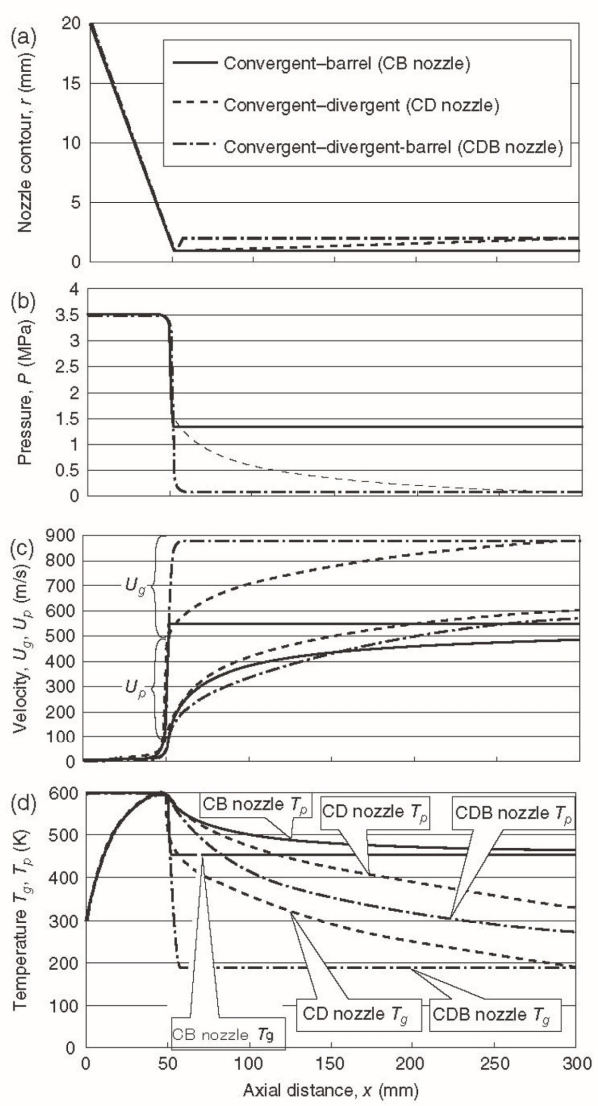

FIGURE 3.15 Effect of nozzle geometry on calculated results of (a) nozzle contour, (b) gas pressure, (c) velocity of gas and particle, (d) temperature of gas and particles for nitrogen as the process gas, copper particle (15 μm). Gas initial (stagnation) pressure P_i=3.5 MPa, gas initial temperature T_{gi} =600 K, gas initial velocity U_{gi} =10 m/s, T_{pi} =300 K, particle initial velocity U_{pi} =10 m/s7[26)].

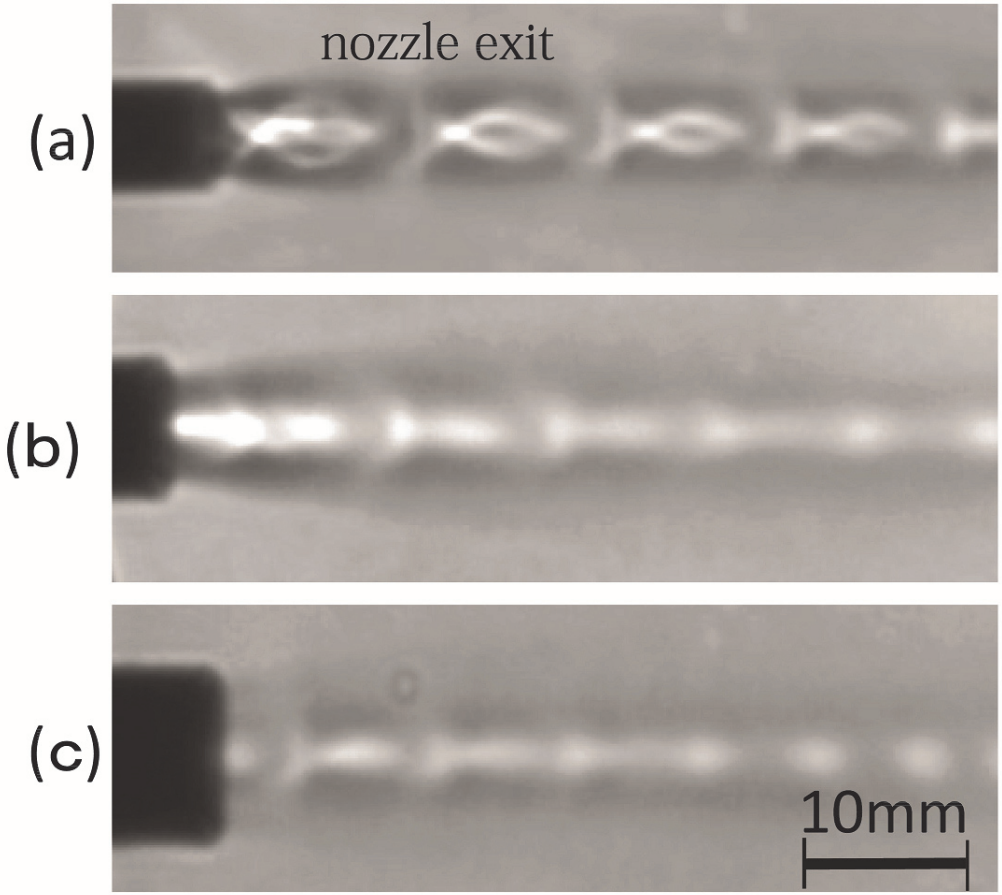

FIGURE 3.16 Schlieren photograph illustrating the influence of the expansion ratio of the nozzle on the expansion state of nitrogen gas jet without substrate. The expansion ratio A_t / A_e of the gun nozzle: (a)4; (b)9, (c)16. (T_{gi} = room temperature, P_i =3.0 MPa)

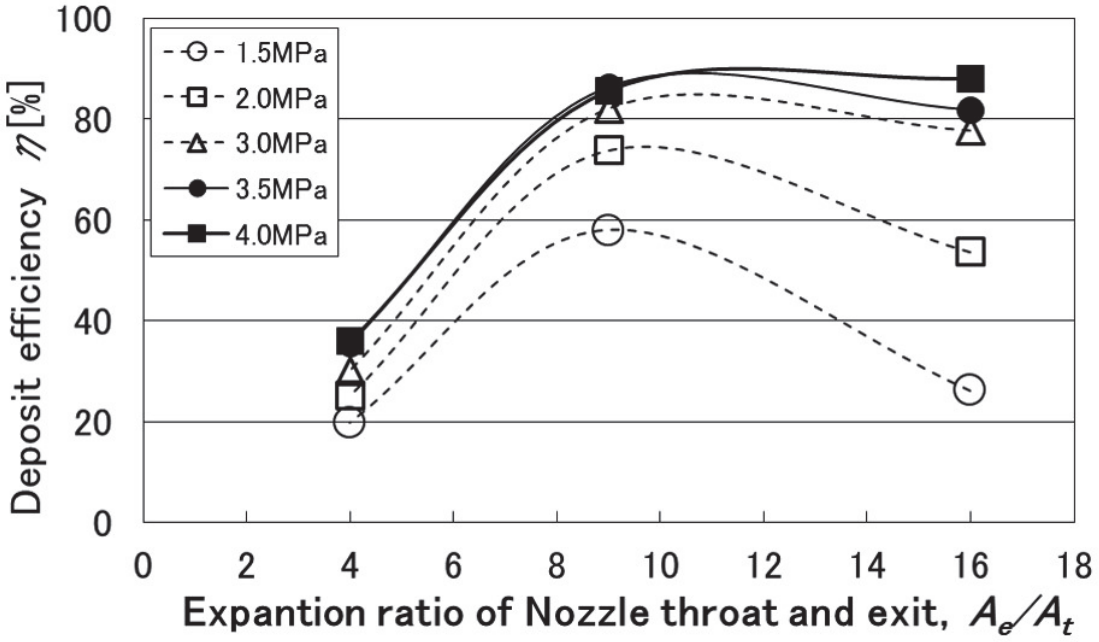

FIGURE 3.17 Influence of the expansion ratio of the gun nozzle and gas pressure on the deposition efficiency of cold sprayed copper (10 μ m) coatings at T_{gi} = 400℃,with powder R/I[33].

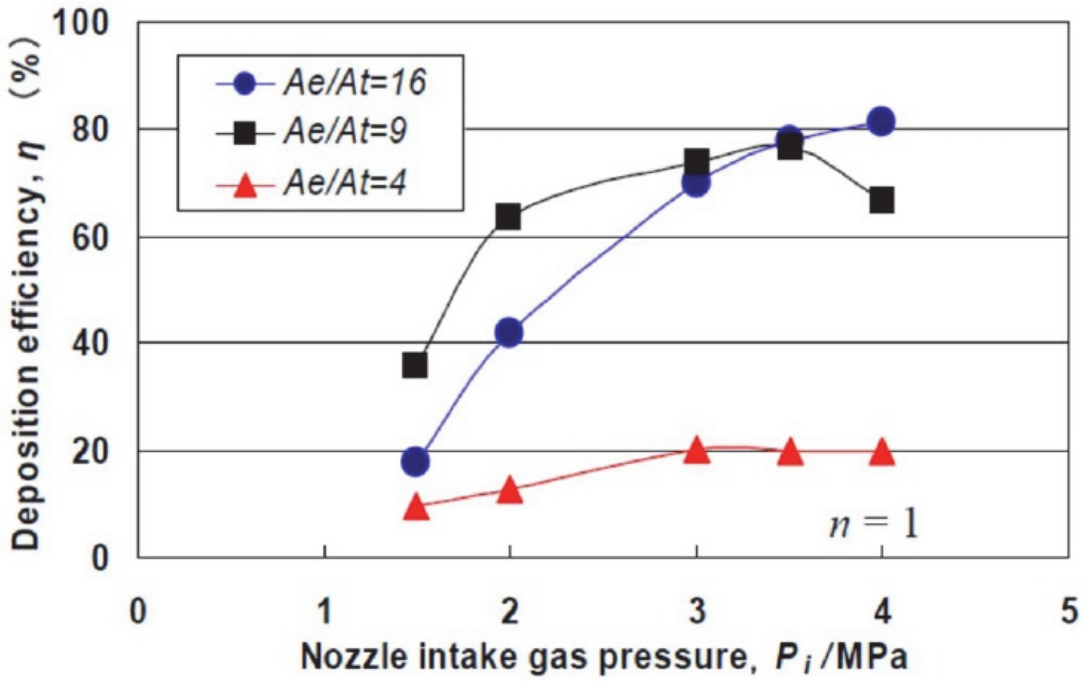

FIGURE 3.18 Influence of the gas pressure and expansion ratio of the gun nozzle on the deposition efficiency of cold sprayed copper (10 μ m) coatings at T_{gi} = 300℃,with powder R/I[33].

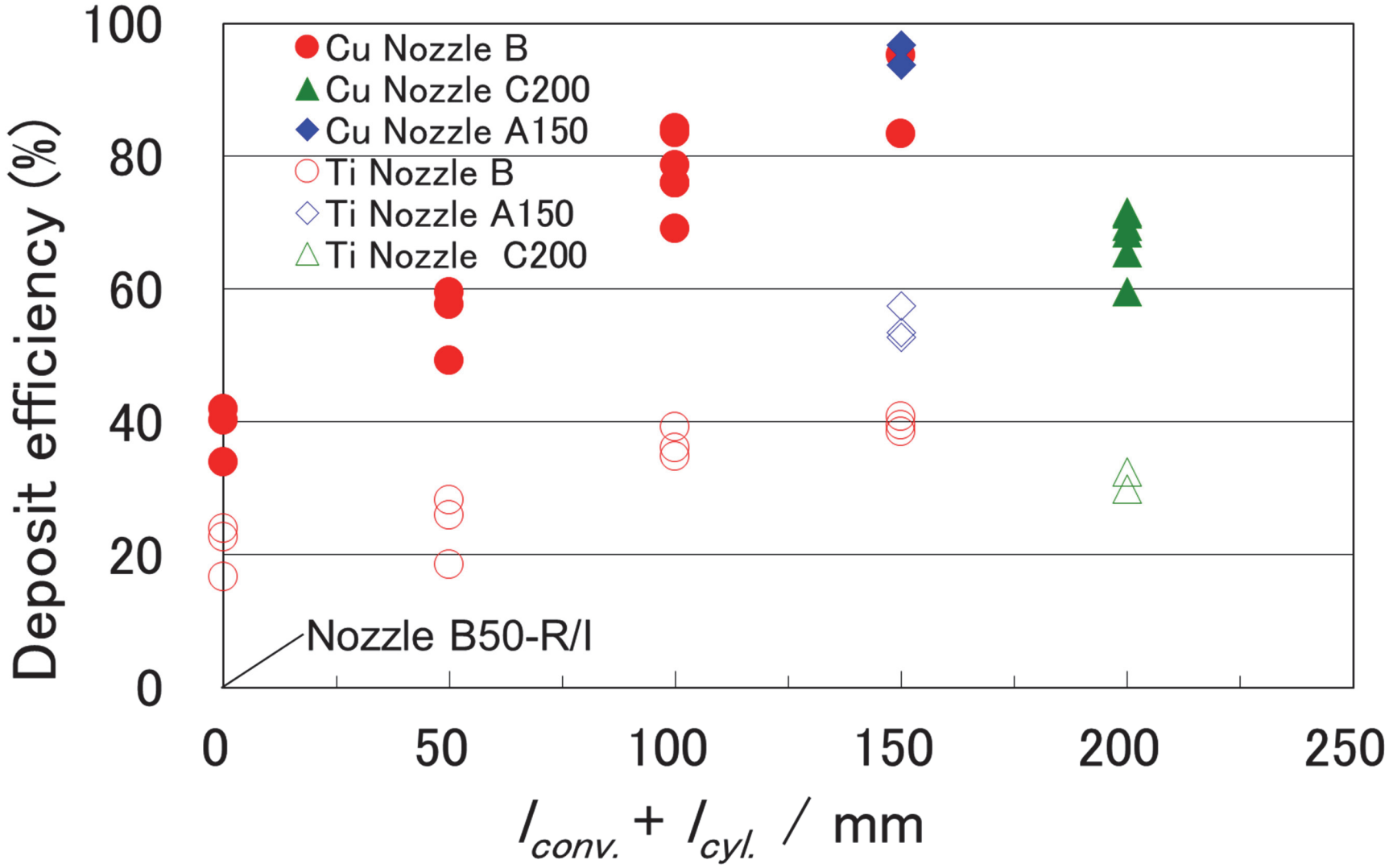

FIGURE 3.19 Effects of entrance convergent section length of nozzle type A(Converging-diverging nozzle), B(Converging-diverging -barrel nozzle) and C(Cylinder-converging-diverging -barrel nozzle) on the depositing efficiency with copper(mean particle size: 13μm) and titanium powder(mean particle size: 25μm) with nitrogen gas initial (stagnation) pressure P_i=3.0 MPa, gas initial temperature T_{gi} =350℃ [32].

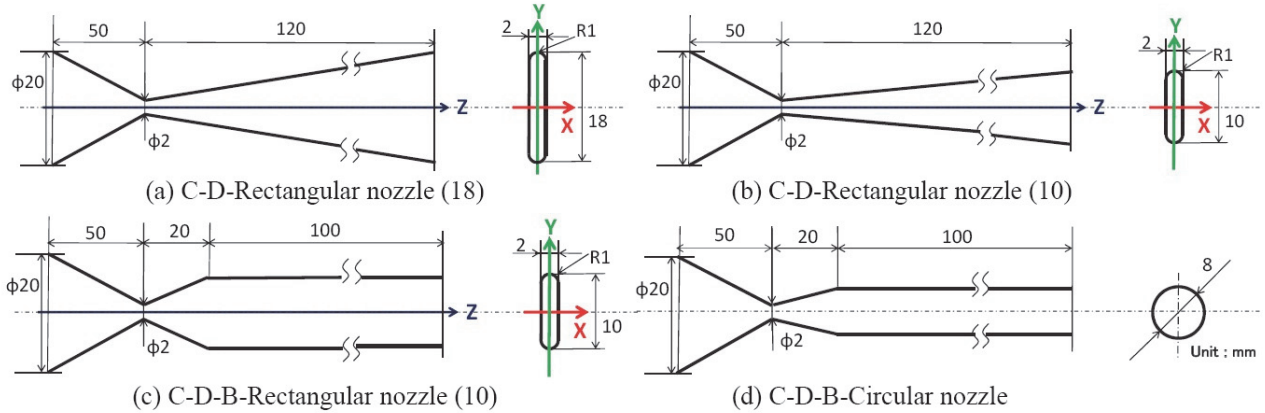

Figure 3.20 Schematic diagrams of rectangular and circle cold spray nozzles[37].

TABLE 3.3. Classification of cold spray process and device.

No.	Type		Process gas			Main characteristic	Commercial device ＜ ＞
			Gas type	Stagnation pressure[MPa]	Stagnation temperature[℃]		
(a)	Cold spray	High press. /low temp.	※	1～ (4)	under 600	First-generation CS device	-developed by researchers <SM Kinetiks 3000>[4] <Taekwang tech(Korea)>[5]
(b)		High press. /high temp.	※	～4(max. 5)	Up to 1000	Second generation CS device Application to fireproof metal	<SM Kinetiks 4000, 8000>[4] <II 5/8,5/11>[6] ＜PG PCS-800, 1000>[7]
(c)		High press. portable	※	1～2	Under 400	Al, Cu, Zn, Ag, etc.	<SM Kinetiks 2000>
(d)		Low press. portable	Air	under 1	(under 600)	·Low melting point metal, ·Repair use	<OCPS(Russia) DYMET 412, 403>[8] <Centerline(Canada) SST>[9]
(e)		Low press. sonic	Helium	under 1	(under 400)	Little gas consumptions, controlled by lower than sound speed	<Inovati(USA) KM-CDS, PCOMCS>[10]
(f)		Low press. / high temp.	※		Under 900		＜Medicoat(Switzerland) ACGS＞[11]
(g)		Shock-wave Induced Spray Process (SISP)	Helium？	2	550-900	Al, Cu. SUS	Developed by Ottawa Univ. at 2005[12]
(h)	Low temp. HVOF	(Low temp. HVOF) Warm spray	Combustion gases + Nitrogen, (air)	(under 1)	(600 - 2000)	Improvement of HVOF, Superior coating of Ti, WC-Co	-developed by researchers -NIMS/Kagoshima Univ. -no commercial device
(i)		High pressure warm spray	Combustion gases + Nitrogen	under 4	1430 - 2350	making warm spray high pressurized, Superior coating of Ti	＜PG/NIMS/Kagoshima Univ.＞[13]

SM：Sulzer Meteco(Switzerland), II：Impact Innovations GmBH(Germany), PG: Plasma Giken Co. Ltd. (Japan),

NIMS：National Institute for Materials Science (Japan)

※：Nitrogen, helium, air or those mixed gases

TABLE 3.4 Nozzle configuration and gas conditions [26].

Table 3.4 Cold spray gun nozzle size

Nozzle No.:	Nozzle geometry	Powder injection position	d_i mm	d_t mm	d_e mm	*expansion ratio of* A_e/A_t	l mm	$l_{conv.}$ mm	$l_{div.}$ mm	$l_{bar.}$ mm
CB: Convergent-barrel nozzle*		Axial	40	2	4	4	300	50	-	250
CD: Convergent-divergent nozzle*		Axial	40	2	4	4	300	50	250	-
CDB: Convergent-divergent-barrel nozzle*		Axial	40	2	4	4	300	50	10	240

*: use in numerical simulations in Figure 3.14.